Analysis of Single and Tandem Cylinder Data Using an Orthogonal Volterra Model Approach

I.A. Sibetheros and J.M. Niedzwecki[*]
Department of Civil Engineering, Texas A&M University
College Station, Texas 77843, USA

Abstract

The development of a definitive predictive model that accurately accounts for the nonlinear hydrodynamics and structural response behavior observed in arrays of closely spaced risers on deep water structures will require a more detailed understanding of this fluid-structure interaction. Through the analysis and interpretation of data from model basin tests on single and paired tandem cylinder configurations this study is directed at uncovering the nature of some aspects of this nonlinear response behavior using an orthogonal third-order Volterra technique that can delineate between linear, quadratic and cubic nonlinear frequency dependent behavior. As part of the analysis procedure the data was organized in input-output pairs that would provide logical groupings of the measured quantities. The data pairs presented in this study include wave excitation and inline cylinder displacement, wave excitation and transverse cylinder displacement, wave excitation and inline reaction force, and, upstream cylinder and downstream cylinder response. This information is presented in terms of spectral and coherence plots. The single cylinder data is presented as a means to contrast the behavior of the tandem cylinders. Both configurations were analyzed at two different pre-tensions adding another dimension to this investigation. It is shown that although a primary variable such as displacement may be more easily measured, pretension and force measurements provide an important key to our understanding of this difficult problem.

Key Words: single cylinder, tandem cylinders, random waves, linear behavior, quadratic behavior, cubic behavior; nonlinear response, orthogonal Volterra model, orthogonal coherence.

[*] Corresponding author. Tel: (979) 862-1463; fax; (979) 845-8986; email: j-niedzwecki@tamu.edu

1. Introduction

In the design of deep water structures, such as tension-leg platforms or spar platforms, long slender flexible cylinders are often clustered due to space and equipment constraints. This presents a serious design challenge since each structural element must be designed for suitable fatigue life targets and in the case of clustered structural elements such as risers, the designer must also take into account possible damage due to flow induced collisions. Unfortunately, reliable and robust predictive models that account for the nonlinear hydrodynamic interactions and coupled response of each individual member in such groups exposed to wave and current flow is not currently available. This situation directly reflects the limited understanding of the hydrodynamic interference effects and the complex nature of this fluid flow field.

Basic small scale experimental studies to investigate the fluid interaction of two or more cylinders in close proximity exposed to oscillating or wave flows were limited to either rigidly-mounted or flexibly-mounted rigid cylinders (e.g. Sarpkaya and Isaacson, 1981; Borthwick and Herbert, 1988; Blevins, 1990; Haritos and He, 1993). The emphasis in those studies was on obtaining wave force transfer coefficients for use in the Morison equation to account for the shielding effect between cylinders. As a result of these studies it was determined that flow interference under certain conditions had significant effects on force coefficients of each individual cylinder within the array. Further it was established that the interference phenomenon is in general a function of flow characteristics, cylinder flexibility, as well as spacing and orientation with respect to flow direction.

A series of larger scale experimental studies examining the wave-induced response of long, flexible vertical cylinders in close proximity were conducted in a deepwater model basin. The first of a series of experiments were performed using a distorted scale technique as reported by Duggal and Niedzwecki (1994b, 1995). In this series of tests effort was focused on developing a probabilistic analysis of the collision behavior of a pair of cylinders in tandem orientation. The relative displacements as a function of elevation within the water column was computed using strain gauge measurements obtained at selected points along the interior of the flexible cylinder models. These displacements were later compared to those predictions obtained using a finite element model. The results confirmed that the magnitude

of the relative displacement was controlled by differences in pretension between the two cylinders leading to changes in structural response amplitude, frequency and phase. Orientation of the cylinders with respect to one another was also explored and some mapping of force changes was presented. Further, ideas related to mild cylinder collisions were suggested by the data (Duggal and Niedzwecki, 1994a). Single scale single cylinder model tests subjected to wave and shear current profiles were next studied by Guérandel (1994). In the most recent set of multiple riser experiments, direct displacements measurements were obtained utilizing underwater optical tracking techniques. An algorithm to resolve the displacements of multiple submerged objects from multiple cameras was developed and presented by Rijken and Niedzwecki (1997). In the study by Rijken (1997) a finite element formulation for a cluster of cylinders under a variety of hydrodynamic loading conditions was implemented based on the work of Paulling and Webster (1986). In comparing the numerical prediction with the experimental results, large differences between the results in clearance estimates were attributed to the lack of an interactive module in the numerical formulation, to account for the experimentally observed interaction behavior.

In an earlier study, the orthogonal Volterra modeling approach was used to investigate the wave-interaction with a flexible horizontal cylinder (Sibetheros, Rijken and Niedzwecki 2000). That study addressed the use of the model and several practical issues encountered in its application. In particular, modeling and prediction error parameters were used to determine the minimum experimental data lengths for the proper estimation of the Volterra transfer functions. The proper use of the estimated Volterra transfer functions for system output predictions under different input excitations was also addressed. In this study the main objective is to use this analysis procedure to gain a better understanding of the frequency dependent non-linear behavior observed in larger scale model basin tests of single and tandem cylinder configurations. To accomplish this goal it is important to identify and quantify the linear and nonlinear relationships between random wave excitation and the force and displacement data corresponding to single and paired cylinder configurations.

2. The Orthogonal Volterra Model

The input-output system presented in Figure 1. can be expressed literally and mathematically as follows (Sibetheros, Rijken, and Niedzwecki 2000). Given the input time series, $x(t)$, of some process of interest and some corresponding output process, *y(t)*, the Volterra modeling objective is to calculate the linear transfer function and non-linear transfer functions such that the approximation obtained is within some acceptable modeling error. This can be expressed in the frequency domain as

$$\begin{aligned}\hat{Y}(f) = H_1(f)X(f) + \sum_{\substack{f_1}}\sum_{\substack{f_2 \\ f_1+f_2=f}} H_2(f_1,f_2)X(f_1)X(f_2) \\ + \sum_{\substack{f_1}}\sum_{\substack{f_2}}\sum_{\substack{f_3 \\ f_1+f_2+f_3=f}} H_3(f_1,f_2,f_3)X(f_1)X(f_2)X(f_3)\end{aligned} \tag{1}$$

with,

$$Y(f) = \hat{Y}(f) + \varepsilon(f) \tag{2}$$

where, $Y(f)$ and $X(f)$ denote the Fourier transforms of $x(t)$ and $y(t)$, and $\hat{Y}(f)$ is the Volterra model output and, $\varepsilon(f)$ is the modeling error. Further, $H_1(f_1)$ is the linear transfer function (LTF), $H_2(f_1,f_2)$ is the quadratic transfer function (QTF), and $H_3(f_1,f_2,f_3)$ is the cubic transfer function (CTF). In Eqn. (1) the second term on the right hand side models the contributions of all frequency pairs present in the input which, as a result of quadratic mixing, add (or subtract) to frequency *f* in the output. The contribution of any particular frequency pair is given by the product of the complex amplitudes $X(f_1)X(f_2)$ multiplied by the quadratic transfer function, $H_2(f_1,f_2)$. Similarly, the third term in Eqn. (1) models the contributions of all frequency triplets present in the input which, as a result of cubic mixing, add (or subtract) to frequency *f* in the output. The contribution of any particular frequency triplet is given by the product of the complex amplitudes $X(f_1)X(f_2)X(f_3)$ multiplied by the cubic transfer function, $H_3(f_1,f_2,f_3)$.

The Volterra model, Eqn. (1), is a very powerful nonlinear system identification tool because it has a canonical form and it is nonparametric. This means that the model does not

require apriori information about the nonlinear characteristics of the actual physical system which is being modeled. The linear and nonlinear transfer functions, in which the linear and nonlinear physics of the unknown system of interest is imbedded, can be estimated by well established higher-order statistical signal processing techniques provided that the random input data are Gaussian. This was a serious practical constraint of the original Volterra model formulation that was removed by the subsequent research developments as reported by Kim and Powers (1988) and Nam and Powers (1994). Their research opened the way for the use of Volterra modeling techniques to address more common real-world problems where the input was non-Gaussian. Even with this issue resolved, there is another problem that arises with the method. The model outputs of the linear, quadratic, and cubic parts are complex quantities and are not orthogonal to each other. This means that the contributions from each transfer function at a given output frequency may act constructively or destructively with one another in the summation of the right-hand side of Eqn. (1) according to the relative phases of the outputs from the various components. The result is the appearance of "interference" terms when using the model of Eqn. 1 to calculate the output power spectrum. In order to avoid these interference effects, which greatly hinder the interpretation of linear and nonlinear phenomena, Im and Powers (1996a, 1996b) developed the orthogonal Volterra model. In their method the input vector is modified to assure orthogonality using the Gram-Schmidt procedure.

Consistent with the orthogonal Volterra model the coherence or total coherence, $\gamma^2(f)$ can be expressed as

$$\gamma^2(f) = \gamma_L^2(f) + \gamma_Q^2(f) + \gamma_C^2(f) \tag{3}$$

where, $\gamma_L^2(f)$ is the linear coherence representing the fraction of the observed response power spectrum at frequency f which can be accounted for by the linear component of the orthogonal Volterra model. Similarly, $\gamma_Q^2(f)$ is the quadratic contribution to the coherence and, $\gamma_C^2(f)$, the cubic coherence contribution. It should be noted that each of the orthogonal coherences in Eqn. 3 is bounded by zero and unity, and that the closer the total coherence $\gamma^2(f)$ is to unity the better the Volterra model approximation of the system output power.

3. Particulars of the Experiments

The single and tandem cylinder model experiments were conducted at the Offshore Technology Research Center model basin. The single and tandem cylinder model tests were performed in the deepest part of the model basin, a deep rectangular pit which is 16.76 m (55 ft) deep. The cylinder arrangement is shown schematically in Figure 1. The cylinder models consisted of a steel wire core tightly covered by an ABS tube. The model scale was 1:75. No instrumentation was placed inside or along the exterior of the cylinder, only small tape markings were placed on the exterior at predetermined elevations for optical tracking. The steel wire core allowed for variations in the pretension loads and the ABS tube created the specified hydrodynamic model diameter. For the tandem cylinder, two identically constructed models were used. In this study the tandem cylinders were spaced at 3.5 diameters, and were evenly pretensioned. Two different pretension cases, corresponding to 9.815 MN and 13.8 MN pretension in prototype scale were selected for analysis. The cylinder diameter of the cylindrical models was 14.2 mm (.5 in) which scales to the prototype dimension of 710 mm (28 in). The prototype water depth was 850 m (2,789 ft) and the cylinder length was 857 m (2,812 ft).

Wave elevation measurements were obtained using five capacitance wave probes in an about the experimental setup. Reaction forces at the top and bottom of each cylinder were from shear strain measurements. Cylinder displacement was characterized by the motion of a single target on each cylinder, which was simply a white tape attached to the cylinder at a point 298 m below the water surface. The two-dimensional position of this target was established from two cameras and a computer algorithm for obtaining the global coordinates of the underwater target based upon digitized data from the cameras (Rijken and Niedzwecki, 1998). The wave environment for the selected data sets represented a 1 hour realization of a 100 year storm in the North Atlantic, characterized by a JONSWAP wave elevation spectrum model with a significant wave height of 14.0 m, a peak period of 16.3 s and a peak enhancement factor of 2.0.

4. Analysis of the data

As part of the analysis procedure the data was organized in input-output pairs that would provide logical groupings of the measured quantities. The data pairs selected for discussion include wave excitation and inline cylinder displacement, wave excitation and transverse cylinder displacement, wave excitation and inline reaction force (sum of the inline reaction forces at top and bottom ends of the cylinder), upstream cylinder and downstream cylinder response. It should be mentioned that transverse reaction force data was not included in the analysis, since the transverse reaction force data at the bottom end of the cylinder was not available due to and instrumentation malfunction. A summary of the input-output pairs that were analyzed are presented in Tables 1, 2 and 3. The first two tables treat all the cases as independent single cylinders cases and establish a common process for dealing with variables of interest as they relate to the input wave elevation spectrum. These include displacement and reaction forces at the two pretension conditions. The third table builds upon this process but now specifically addresses the interaction of the upstream and downstream cylinders that will be examined in the figures defined in Tables 4 and 5. The six figure composite presentation of the data analysis is outlined for both the analysis of all the data in the single cylinder format and in the tandem interaction format.

Care has been taken to present the analysis of the data in a form that is more easily interpreted for gaining insight into the nature of the physical processes. In particular, log scales for spectral amplitude are not used and the coherence plots separate out the linear, quadratic and cubic contributions for ease of interpretation. The total coherence was included to provide guidance on the total strength of the combined contributions to model the specific data being analyzed. The single cylinder tests are used for the baseline in the comparison with the data on the pair of tandem cylinder responses. The idea of treating all cases as single cylinders is investigated and contrasted with the graphical interpretation of the interaction between the tandem cylinder pair.

4.1 Wave elevation- inline cylinder displacement pair

The results of the wave elevation-inline cylinder displacement system analysis for the single and the paired cylinder configurations are presented in the composite Figures 3 and 4 for pretension (T) equal to 9.815 MN and 13.8 MN, respectively. In each graph results are

presented for “three” cylinder cases, that is the single cylinder, and the upstream and downstream tandem cylinders, considered and analyzed as single cylinders with respect to the wave excitation. The power spectral densities (Figures 3(b) and 4(b)) for the single and tandem cylinders are very similar in both pretension cases, with the exception of the downstream tandem cylinder for T= 13.8 MN displaying lower peak and higher zero frequency (mean) spectral values. It appears that the upstream tandem cylinder responds to the wave excitation like the single cylinder, with regards to their inline displacement amplitude. On the other hand, the presence of the upstream cylinder affects the downstream cylinder’s inline displacement auto-power spectrum, particularly in the higher pretension case.

The orthogonal coherence spectra in Figures 3(c)-(f) for T=9.815 MN and 4(c)-(f) for T=13.8 MM display the fractions of the observed response (inline cylinder displacement) power accounted for by the Volterra model as a whole, and by each of its linear, quadratic, and cubic components, respectively. The total coherence spectra for the three wave-cylinder systems are very similar, particularly over the high energy frequency band (0.02 Hz to 0.17 Hz), with average values of 0.80 (80%) or higher over this frequency band. The linear coherence spectra, too, are very similar in both pretension cases with average values of 0.50 (50%) or higher over the same frequency band (Figures 3(d) and 4(d)). The quadratic coherence spectra (Figures 3(e) and 4(e)), on the other hand, have very low values over the same frequency band, with higher values at low (difference) and high (sum) frequencies. The cubic coherence spectra (Figures 3(f) and 4(f)) have average values of 0.25 (25%), approximately, over the [0.02-0.17 Hz] frequency band, and higher values at low and high frequencies.

It is worth noting for modeling purposes that, for each of the three wave-cylinder systems the linear component of the Volterra model contributes about 80% of the model output (inline cylinder displacement) power for T=9.815 MN, over the high wave energy frequency band, with the other 20% being contributed mainly by the cubic component. For T=13.8 MN, the linear component contributes around 70% and the cubic component approximately 30% of the model output power, respectively, over the high wave energy

frequency band.

The high total coherence values in Figures 3 and 4 for the three wave-cylinder systems suggest that the wave excitation-inline cylinder displacement relationship can be adequately modeled by a third-order frequency domain Volterra model, with the main contribution coming from the model's linear component. Furthermore, the strong similarity of the linear and nonlinear composite coherence spectra for the three wave-cylinder systems indicates that these systems have very similar linear/nonlinear characteristics. Taking also into account the similarity of the auto-power spectra for the inline displacements, which was discussed earlier, it can be argued that each of the tandem cylinders responds to the wave excitation, in terms of its inline displacement, in the same manner as the single cylinder. The above results, however, do not directly address the nature of the interaction between the two tandem cylinders, and do not provide information on whether the two tandem cylinders respond in phase with regards to their inline displacement. In order to address these issues an upstream-downstream cylinder response analysis was performed using Volterra modeling. It is discussed in Section 4.4.

4.2 Wave elevation- transverse cylinder displacement pair

The results of the wave elevation- transverse cylinder displacement data analysis are displayed in the composite Figures 5 and 6, for T=9.815 MN and 13.8 MN, respectively. They are markedly different than the inline displacement analysis results discussed in the previous section. The auto-power spectra for the transverse displacements (Figures 5(b) and 6(b)) reveal large differences between the tandem cylinders and the single cylinder in both pretension cases, and between the upstream and the downstream tandem cylinders for T=9.815 MN. The downstream tandem cylinder for T=9.815 MN and both tandem cylinders for T=13.8 MN have significant spectral values only at very low frequencies. This indicates that, in these cases the transverse displacement measured time series comprise of a large steady component and a small time-varying component.

The coherence spectra for the three wave-cylinder systems for T=9.815 MN (Figures 5(c)-(f)) are very similar, with total coherence about 0.50 (50%). The linear and quadratic

coherence spectra are close to zero, with the exception of the linear coherence for the wave-single cylinder system, which has an average value of 0.12 (12%), approximately, over the [0.05-0.10] Hz frequency band. The cubic coherence spectra, on the other hand, are very similar to the total coherence spectra, suggesting that the output of the cubic component of the Volterra model is the main contributor to the modeled output (transverse displacement) power.

It is very interesting to note that, although the transverse displacement auto-power spectrum of the upstream cylinder (Figure (5(b)) peaks in the band centered at around 0.07 Hz, which is within the high wave energy frequency band (Figure 5(a)), the linear coherence spectrum (Figure 5(d)) does not detect any linear correlation between the wave excitation and the transverse displacement of the upstream tandem cylinder. This case is a good example of the effectiveness of Volterra modeling in detecting and quantifying linear and nonlinear correlations between measured input data and simultaneously measured output data of an unknown physical system.

The total coherence spectra for the two wave-tandem cylinder systems for T=13.8 MN (Figure 6(c)) display high values at frequencies close to zero, which are mainly due to the quadratic component of the model as indicated by the quadratic coherence spectra depicted in Figure 6(e). These results also suggest that the high auto-power spectral values at frequencies close to zero for the tandem cylinders (Figure 6(b)) are mainly a product of quadratic nonlinear (difference frequency) interactions between wave excitation spectral components. It is interesting to note that such quadratic nonlinear interactions were not detected in the wave-single cylinder system in both pretension cases, and in the wave-tandem cylinder systems for T=9.815 MN.

The transverse displacement results indicate differences between the tandem cylinders' transverse response for T=9.815 MN, and between the tandem cylinders and the single cylinder in both pretension cases. Furthermore, the transverse displacements for all three wave-cylinder systems are not linearly related to the wave excitation, and cannot be modeled by third-order Volterra models as well as the inline displacements. It can be

concluded that in the tandem cylinder configuration interference phenomena have a stronger effect on the transverse response than on the inline response behavior.

4.3 Wave elevation- inline cylinder reaction force pair

Figures 7 and 8 depict the wave elevation-inline cylinder reaction force results for the three wave-cylinder systems for T=9.815 and 13.8 MN, respectively. The auto-power spectra for T=9.815 MN (Figure 7(b)) have a single peak at around 0.07 Hz, which coincides with the peak of the wave elevation auto-power spectrum, suggesting a linear correlation. The auto-power spectrum for the upstream cylinder has higher power content than the other two auto-power spectra for frequencies higher than 0.07 Hz. Furthermore, the downstream cylinder has a higher peak at 0.07 Hz than the other cylinders, which have identical peaks. The auto-power spectra for T=13.8 MN (Figure (8(b)), too, have a peak at around 0.07 Hz, suggesting a linear correlation with the wave excitation, and another peak of similar magnitude at zero frequency, suggesting a quadratic (difference frequency) correlation with wave excitation. Contrary to the lower pretension case, the single cylinder has the highest peak at 0.07 Hz, followed closely by the upstream cylinder, and by the downstream cylinder which has the lowest peak (around 16% lower than the upstream cylinder's peak).

The coherence spectra in Figures 7(c)-(f) for T=9.815 MN suggest that the upstream cylinder's response deviates from the strong correlation with the wave excitation that characterizes the other two cylinders' response. For example, the total coherence for the upstream cylinder has an average value of around 0.8 (80%) over the [0.03-0.12] Hz, compared to an average value for the other two cylinders exceeding 0.96 (96%) over the same frequency band (Figure 7(c)). The linear coherence for the upstream cylinder has an average value of around 0.52 (52%) over the [0.03-0.12] Hz frequency band, compared to an average value for the other two cylinders of around 0.85 (85%) over the same band (Figure 7(d)). The quadratic coherence for all three cylinders is very low over the [0.03-0.12] Hz band, where most of the response power lies. The cubic coherence for the upstream cylinder has an average value of about 0.25 (25%) over the same band, whereas the cubic coherence for the other cylinders is very low.

The coherence spectra for T=13.8 MN (Figures 8(c)-(f)) for the three wave-cylinder systems are almost identical in the [0.03-0.12] Hz frequency band, with average total coherence values exceeding 0.95 (95%), and average linear coherence values exceeding 0.85 (85%). It can be therefore concluded that within this frequency band the inline reaction forces for the three wave-cylinder systems are strongly linearly related to the wave excitation. The quadratic coherence spectra have values close to zero in the [0.03-0.12] Hz, but have values of 0.75 (75%) for the single cylinder, 0.50 (50%) for the upstream cylinder, and 0.32 (32%) for the downstream tandem cylinder at zero frequency. These quadratic coherence results suggest that the auto-power spectra peaks for the single and to a lesser extent for the upstream tandem cylinders at zero frequency (Figure 8(b)) can be attributed to quadratic (difference frequency) interactions between wave excitation spectral components at select frequencies. The downstream cylinder's zero frequency response on the other hand appears to be the result of both quadratic and cubic interactions, each contributing approximately half of the model's output power, which however is only 62% of the measured output power (Figure 8(c)).

The above results indicate that the pretension level has a more pronounced effect on the inline cylinder reaction force and its relationship to wave elevation than on the inline cylinder displacement. The pretension level controls the degree of interaction between the two tandem cylinders, which affects their hydrodynamic loading and dynamic response. This may explain the pretension's stronger effect on the inline reaction force (sum of top end and bottom end cylinder reaction forces), which represents each cylinder's integrated inline response to hydrodynamic loading, than on the inline cylinder displacement, which represents the displacement of a single target point on each cylinder.

4.4 Upstream-Downstream Tandem Cylinder Interactions

The purpose of the Volterra modeling of the upstream cylinder-downstream tandem cylinder response system was not to identify and quantify an excitation-response relationship, which was the purpose of the analysis of the wave-cylinder systems detailed in Tables 1 and 2. The two cylinders of the paired cylinder configuration are not directly related in an excitation-response manner, but their responses may be correlated due to the interference or

hydrodynamic coupling between the two cylinders. The paired cylinder response correlation was therefore analyzed by applying the Volterra modeling technique to the upstream-downstream cylinder response data pairs. In this case, orthogonal coherence spectra and magnitude and phase spectra for the linear transfer function were used to present the Volterra modeling results. The linear transfer function results were intentionally picked for presentation, because they allow for a direct assessment of the degree of the cylinder pair's response as a bundle, that is the two cylinders responding in-phase and with similar magnitudes.

The Volterra modeling results for the upstream-downstream cylinder inline displacement pair are presented in Figures 9(a)-(c) for T=9.815 MN, and 9(d)-(f) for T=13.8 MN. It should be noted that the auto-power spectra for the two-cylinder inline displacements were presented in Figures 3(b) for T=9.815 MN and 4(b) for T=13.8 MN. The coherence spectra in Figures 9(a) and 9(d) depict a high total coherence for both pretension conditions, dominated by its linear component with values exceeding 0.90 or 90% over the high wave energy frequency band. The cubic and quadratic coherences have meaningful values only at low and high frequencies. This is, however, of little practical significance, since the power spectral densities for the inline displacements are low at frequencies lower than 0.03 Hz (with the exception of the downstream cylinder inline displacement for T=13.8 MN at very low frequencies) and higher than 0.12 Hz.

The magnitude spectra of the linear transfer function in Figures 9(b) for T=9.815 MN and 9(e) for T=13.8 MN show an average value close to unity over the [0.03-0.12 Hz] frequency band. The phase spectra in Figures 9(c) for T=9.815 MN and 9(f) for T=13.8 MN show phase angles smaller than 10 degrees over the same frequency band. These results suggest that the two-cylinder displacements are strongly linearly related, have similar magnitudes and are in-phase. In other words, for both pretension conditions the cylinder pair responds as a bundle, at least with regards to the inline cylinder displacements.

The two-cylinder inline reaction force analysis results are presented in Figures 10(a)-(c) for T=9.815 MN, and 10(d)-(f) for T=13.8 MN. The auto-power spectra for the two-cylinder inline reaction forces were presented in Figures 7(b) for T=9.815 MN and 8(b) for

T=13.8 MN. The coherence plots in Figures 10(a) for T=9.815 MN and 10(d) for T=13.8 MN display some marked differences. The total coherence for T=9.815 MN is over 0.75 or 75% over most frequencies, but it only reaches 0.9 or 90% at around 0.085 Hz. The linear coherence has a peak value of 0.7 or 70% at the same frequency, with an average value of 0.55 or 55% over the [0.03-0.12 Hz] frequency band. The cubic coherence has an average value of approximately 0.25 or 25% over the same frequency band. It is worth noting the high value (0.5 or 50%) of the quadratic coherence at zero frequency. The total coherence for T=13.8 MN exceeds 0.98 or 98% over the [0.03-0.12 Hz] frequency band, and is exclusively due to the linear component.

The magnitude and phase spectra in Figures 10(b)-(c) for T=9.815 MN and 10(e)-(f) for T=13.8 MN illustrate the stronger linear correlation between the two-cylinder reaction forces in the higher pretension case. For T=13.8 MN the magnitude of the linear transfer function is over 0.95 over the [0.03-0.12 Hz] frequency band, and the phase spectrum shows a phase angle smaller than 5 degrees over the same frequency band. On the other hand, for T=9.815 MN the average magnitude of the linear transfer function is approximately 0.65 over the [0.03-0.12 Hz] frequency band, and the phase angle fluctuates from –10 degrees to +25 degrees over the same frequency band.

It can be concluded that in the case of the two-cylinder inline reaction force correlation, the pretension effect is more pronounced that in the two-cylinder inline displacement correlation. In the higher pretension case, the paired cylinders act as a bundle with regards to their inline reaction forces, which are in-phase and have similar magnitudes. Interference between the two cylinders appears limited. In the lower pretension case, interference between the two-cylinders appears more pronounced. The linear correlation is not as strong as it is in the higher pretension case, and there is larger phase difference between the two-cylinder inline reaction forces. Also, the nonlinear content in the coherence spectrum is higher in the lower than in the higher pretension case, suggesting stronger nonlinear correlations in the former case than in the latter case.

5. Summary and Conclusion

The nonlinear response behavior of closely spaced long flexible cylinders,

representing risers or tendons, exposed to random ocean waves was investigated by utilizing measured data sets from model basin experiments on single and paired cylinders in close tandem formation. A Volterra model approach was used to simulate the input-output relationships between wave excitation and cylinder response. The tandem cylinders were analyzed as single cylinders. In this manner, three wave-cylinder systems were considered, that is wave-single cylinder, wave-upstream tandem cylinder, and wave-downstream tandem cylinder systems. For each wave-cylinder system, the available wave excitation and cylinder response data were organized in input-output pairs. Wave elevation-inline displacement, wave elevation-transverse displacement, and wave elevation-inline reaction force data pairs were fitted with third-order frequency domain orthogonal Volterra-like models. These models, which are an extension of the original Volterra models, are valid for nonGaussian random inputs and by virtue of their orthogonality allow for a direct assessment of the contribution of each of their linear and the nonlinear terms to the simulation of the unknown physical system. Orthogonal coherence spectra were estimated for the each of the Volterra models of the excitation-response pairs. These coherence spectra are very important in system analysis because they illustrate the fractions of the measured response power which are simulated by the Volterra model as a whole, and by each of its constituent linear, quadratic, and cubic components. Auto-power spectra and orthogonal coherence spectra for the wave excitation-upstream and wave excitation-downstream tandem cylinder response systems were compared to one other, and against the auto-power spectra and orthogonal coherence spectra for the wave excitation-single cylinder response system. This comparison allowed for an assessment of the tandem cylinders' interference and pretension level effects on the dynamic response characteristics of each tandem cylinder and on its wave excitation–cylinder response relationship separately. The interaction between the two tandem cylinders was also investigated, by organizing the upstream and downstream cylinder response data in input-output pairs. In this case, the objective was to determine the nature of the correlation and the phase relationship between the two-cylinder responses, and the effect of the pretension level.

Judging from the analysis, it can be concluded that when the cylinder response is represented by its inline displacement, there is little interaction between the two tandem

cylinders and their response does not differ significantly from the single cylinder response. The wave elevation-inline cylinder displacement relationships are also very similar, as revealed by the Volterra analysis of the excitation-response data pairs. The inline displacements of the tandem cylinders are strongly linearly related to each other, and are practically in-phase. These conclusions are valid in both pretension cases. On the other hand when the cylinder response is analyzed in terms of its inline reaction force, the results depend on the level of pretension. In the higher pretension case, the inline reaction forces for the three cylinders and their relationships to the wave excitation are similar. The inline reaction forces for the tandem cylinders are also strongly linearly related to each other and in-phase. However, in the lower pretension case there are marked differences between the responses of the three cylinders and their correlations to the wave elevation. Furthermore, the inline reaction forces for the tandem cylinders are not strongly linearly related to each other and they have a noticeable phase difference. Clearly, the interaction between the tandem cylinders is more pronounced in the lower than in the higher pretension case, and the interaction level affects more the inline cylinder reaction forces than the inline cylinder displacements. The pretension level also affects more the transverse cylinder displacements than the inline displacements. In the lower pretension case the transverse displacements for the three cylinder cases have different auto-power spectra, whereas in the higher pretension case the two tandem cylinders have similar auto-power spectra, which, however differ significantly from the auto-power spectrum for the single cylinder. Furthermore, the wave excitation and transverse displacement data are very weakly linearly related in all three cylinder cases.

ACKNOWLEDGEMENTS

The senior writer gratefully acknowledges the partial financial support of the Offshore Technology Research Center, the Minerals Management Service, and the R. P. Gregory '32 Endowment during this study. He would also like to recognize the support of the National Science Foundation during the performance of the original model test program, and Shell Oil Company for providing the cylinder models for the laboratory experiments.

REFERENCES

Blevins, R.D. (1990). *Flow-Induced Vibration*, Van Nostrand Reinhold Company, New York, NY.

Borthwick, A.G.L., and Herbert, D.M. (1988). "Loading and Response of a Small Diameter Flexibly Mounted Cylinder in Waves, " *J. Fluids and Structures,* Vol. 2, 479-501.

Duggal, A.S., and Niedzwecki, J.M. (1994a). "Probabilistic Collision Model for a Pair of Flexible Cylinders," *J. Applied Ocean Research*, Vol. 16, 165-175.

Duggal, A.S., and Niedzwecki, J.M. (1994b). "Estimation of Flexible Cylinder Displacements in Wave-Basin Experiments," *J. Experimental Mechanics*, September, 233-244.

Duggal, A.S., and Niedzwecki, J.M. (1995). "Dynamic Response of a Single Flexible Cylinder in Waves," *ASME J. Offshore Mechanics and Arctic Engineering*, Vol. 117, 99-104.

Haritos, N., and He, Y.Q. (1993). "Wave Force and Flow Interference Effect on Vertical Cylinders," *Proc. 12th Offshore Mechanics and Arctic Engineering Conference*, ASME, Vol. I, 73-82.

Guerandel, V.L (1994). "Experimental Study of a Single Riser in Waves and Currents," supervised by J.M. Niedzwecki, *Offshore Technology Research Center*, Report 9/94-A6275, October, 111 pp.

Im, S.B., and Powers, E.J. (1996a). "Sparse Models of the Nonlinear Response of a Spar in Random Seas" *Proc. 6th International Offshore and Polar Engineering Conference*, ISOPE-96, Los Angeles CA.

Im, S.B., and Powers, E.J. (1996b). "A Sparse Third-order Orthogonal Frequency-domain Volterra-like Model, "*J. Franklin Institute*, Vol. 333(B), (3), 385-412 (Special issue on Higher-Order Statistics in Signal Processing).

Kim, K.I., and Powers, E.J. (1988). "A digital Method of Modeling Quadratically Nonlinear Systems with a General Random Input, "*IEEE Transactions ASSP*, Vol. 36, No. 11, 1758-1769.

Nam, S.W., and Powers, E.J. (1988). "Application of Higher-order Spectral Analysis to Cubically-Nonlinear System Identification," *IEEE Transactions on Signal Processing*, Vol. 42, No. 7, 1746-1765.

Niedzwecki, J.M., Rijken, O.R., and Soemantri, D.S. (1995). "Dynamic Behavior of Tendons in Random Seas," *Proc. 14th Offshore Mechanics and Arctic Engineering Conference*, ASME, Vol. I(B), 383-392.

Niedzwecki, J.M., and Duggal, A.S. (1993). "Collision Mechanisms and Behavior of a Pair of Long, Flexible Cylinders in Close Proximity," *Proc. 12th Offshore Mechanics and Arctic Engineering Conference*, ASME, Vol. I, 291-298.

Paulling, J.R., and Webster, W.C. "A Consistent, Large-Amplitude Analysis of the Coupled Response of a TLP and Tendon System," *Proc. 9th Offshore Mechanics and Arctic Engineering Conference*, ASME, Vol. III, 126-133.

Rijken, O.R., and Niedzwecki, J.M. (1998). "Direct Displacement Measurements of Submerged Objects," *J. Ocean Engineering,* April/May, Vol. 25, No. 4-5, 309-321.

Rijken, OR (1997). "Dynamic Response of Marine Risers and Tendons, " supervised by J.M. Niedzwecki, *OTRC report 5/97A9175*, May, *Offshore Technology Research Center*, College Station, TX, 128 pp.

Sarpkaya, T., and Issacson, M. (1981). *Mechanics of Wave Forces on Offshore Structures*," Van Nostrand Reinhold Company, New York, NY.

Sibetheros, I.A., Rijken, O.R., and Niedzwecki, J.M. (2000). "Volterra Series-Based System Analysis of Random Wave Interaction with a Horizontal Cylinder," *J Ocean Engineering,* Vol. 27, 241-270.

Wave-Single Cylinder Data Pairs		
Input	**Output**	
Elevation	Inline Displacement	T=9.815 MN
Elevation	Inline Displacement	T=13.8 MN
Elevation	Transverse Displacement	T=9.815 MN
Elevation	Transverse Displacement	T=13.8 MN
Elevation	Inline Reaction Force	T=9.815 MN
Elevation	Inline Reaction Force	T=13.8 MN

Table 1. Summary of the single cylinder systems analyzed.

Wave-Upstream Cylinder Data Pairs			Wave-Downstream Cylinder Data Pairs		
Input	**Output**		**Input**	**Output**	
Elevation	Inline Displacement	T=9.815 MN	Elevation	Inline Displacement	T=9.815 MN
Elevation	Inline Displacement	T=13.8 MN	Elevation	Inline Displacement	T=13.8 MN
Elevation	Transverse Displacement	T=9.815 MN	Elevation	Transverse Displacement	T=9.815 MN
Elevation	Transverse Displacement	T=13.8 MN	Elevation	Transverse Displacement	T=13.8 MN
Elevation	Inline Reaction Force	T=9.815 MN	Elevation	Inline Reaction Force	T=9.815 MN
Elevation	Inline Reaction Force	T=13.8 MN	Elevation	Inline Reaction Force	T=13.8 MN

Table 2. Summary of the analysis of the tandem cylinder cases analyzed as single cylinder systems.

Upstream -Downstream Cylinder Data Pairs			
Input	**Output**		
Upstream Cyl.	Downstream Cyl.	Inline Displacement	T=9.815 MN
Upstream Cyl.	Downstream Cyl.	Inline Displacement	T=13.8 MN
Upstream Cyl.	Downstream Cyl.	Inline Reaction Force	T=9.815 MN
Upstream Cyl.	Downstream Cyl.	Inline Reaction Force	T=13.8 MN

Table 3. Summary of the tandem cylinder cases analyzed to investigate cylinder interaction effects.

Plot	Content
(a)	Wave elevation power spectra density
(b)	Single , upstream and downstream cylinder power spectral densities
(c)	Total coherence spectra for wave-single cylinder, wave-upstream cylinder, and wave-downstream cylinder systems
(d)	Linear coherence spectra for wave-single cylinder, wave-upstream cylinder, and wave-downstream cylinder systems
(e)	Quadratic coherence spectra for wave-single cylinder, wave-upstream cylinder, and wave-downstream cylinder systems
(f)	Cubic coherence spectra for wave-single cylinder, wave-upstream cylinder, and wave-downstream cylinder systems

Table 4. Description of graphical information for single and tandem cylinder cases analyzed as single cylinders, this includes Figures 3 through 8.

Plot	Content
(a)	Total coherence spectra for the upstream-downstream cylinder system T = 9.815 MN
(b)	Magnitude of linear transfer function for the upstream-downstream cylinder system T = 9.815 MN
(c)	Phase of linear transfer function for the upstream-downstream cylinder system T = 9.815 MN
(d)	Total coherence spectra for the upstream-downstream cylinder system T = 13.8 MN
(e)	Magnitude of linear transfer function for the upstream-downstream cylinder system T = 13.8 MN
(f)	Phase of linear transfer function for the upstream-downstream cylinder system T = 13.8 MN

Table 5. Description of graphical information investigating the tandem cylinder interaction effects, this includes Figures 9 and 10.

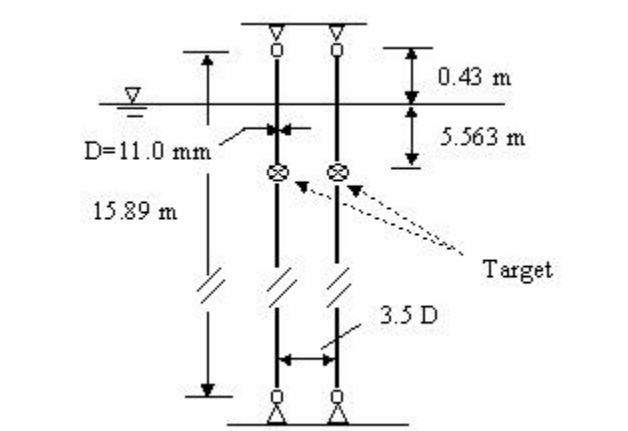

Figure 2. Schematic of the experimental setup for the cylinders in the model basin.

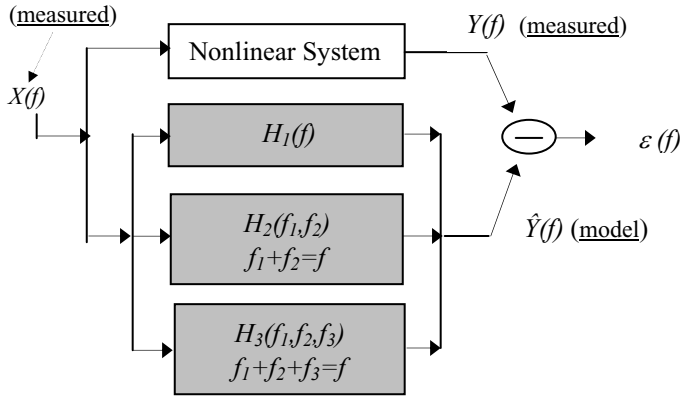

Figure 1. Schematic of the frequency domain Volterra model for a nonlinear system with linear, quadratic and cubic components.

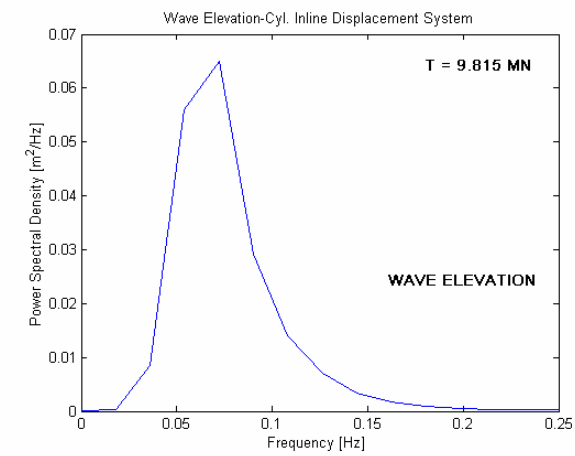

(a)

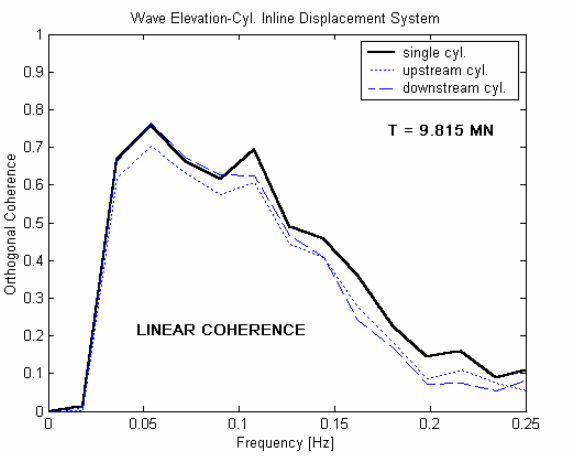

(d)

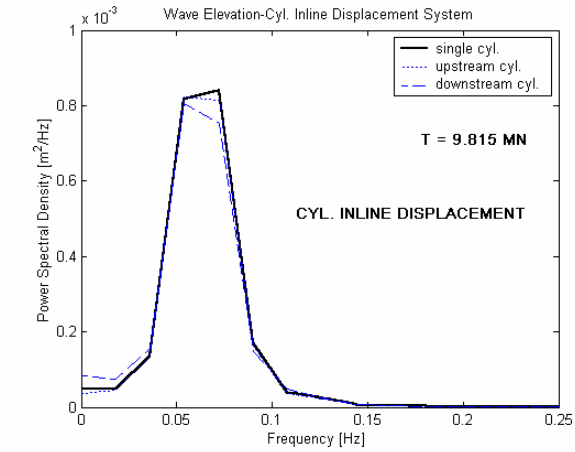

(b)

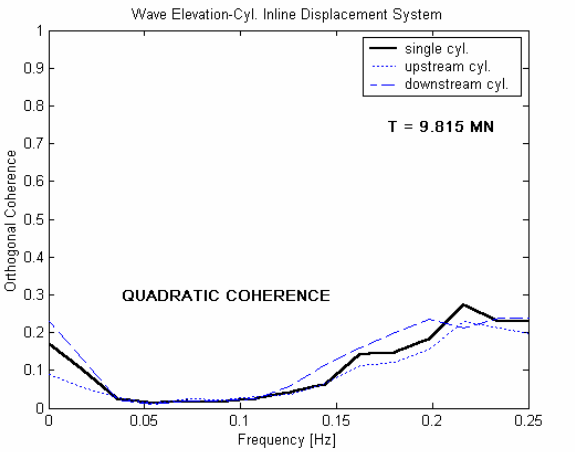

(e)

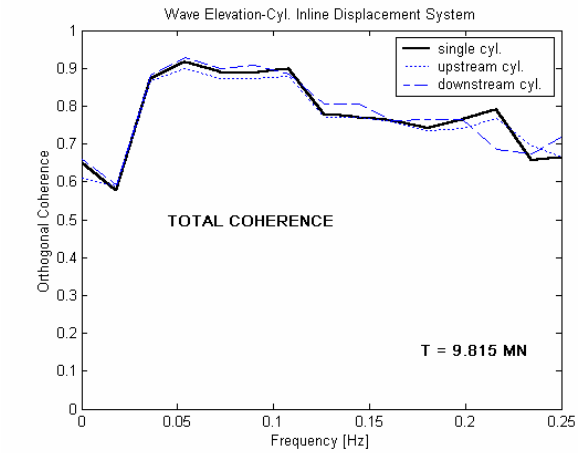

(c)

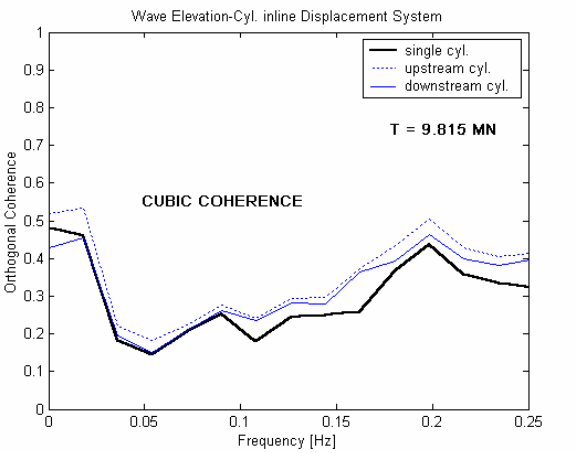

(f)

Figure 3. Volterra Modeling Results for Wave Elevation-Cyl. Inline Displacement Systems; T=9.815 MN.

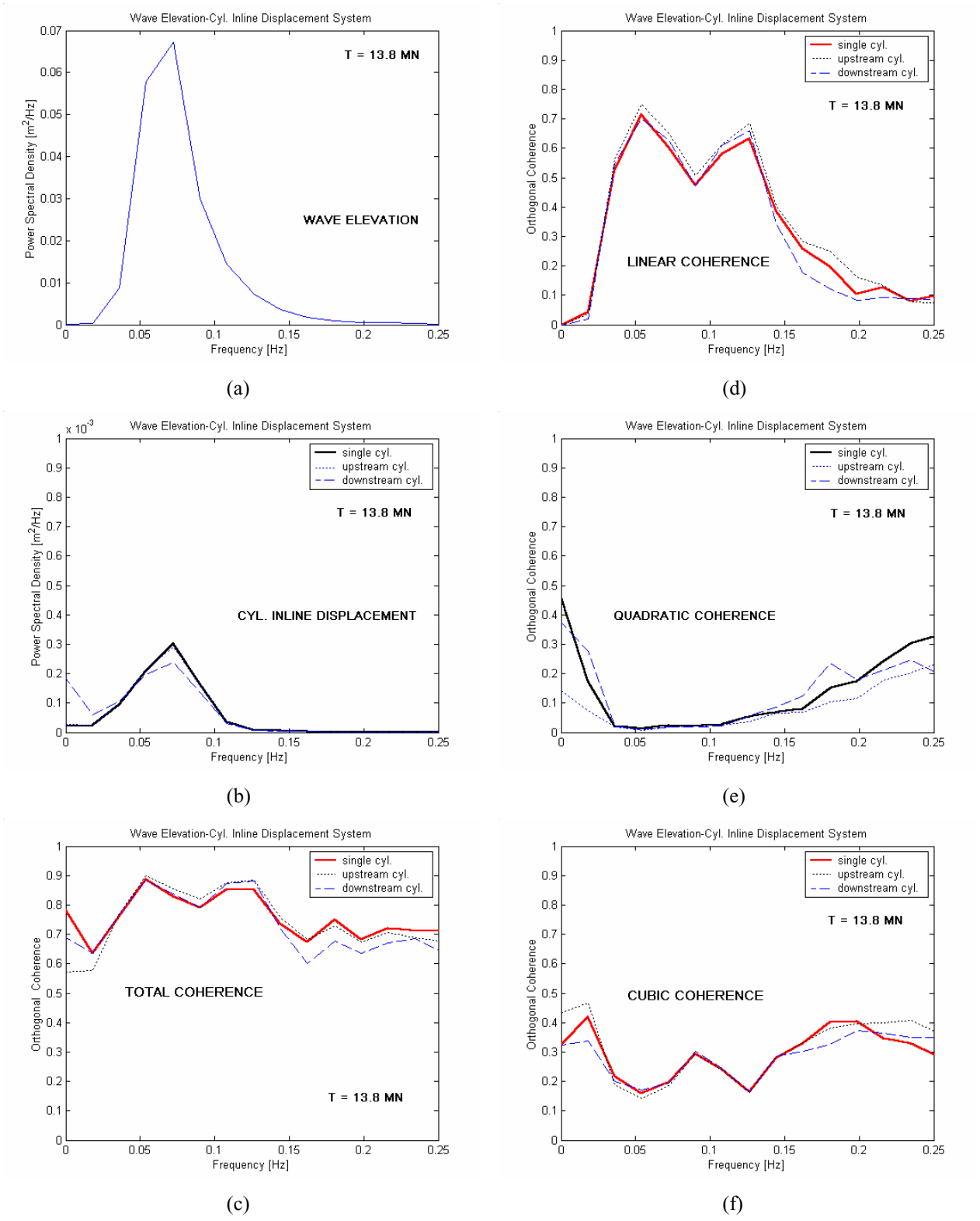

Figure 4. Volterra Modeling Results for Wave Elevation-Cyl. Inline Displacement Systems; T=13.8 MN.

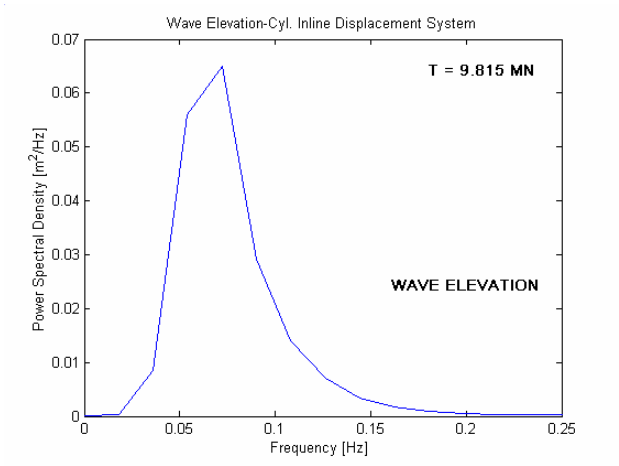

(a)

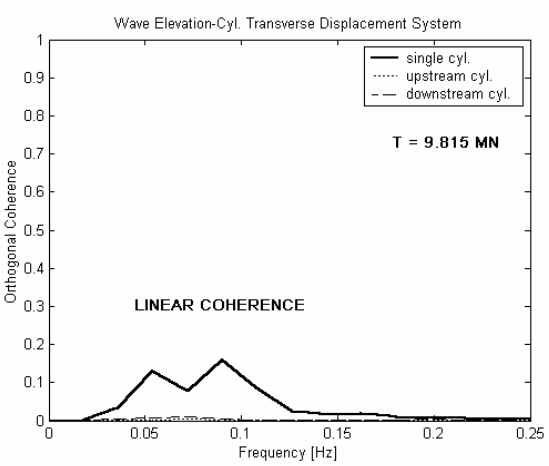

(d)

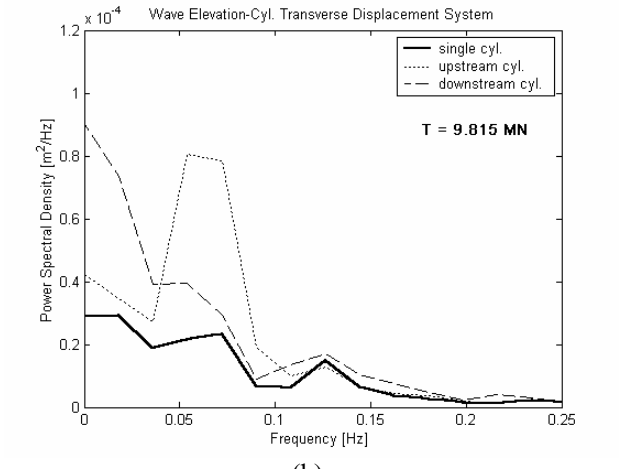

(b)

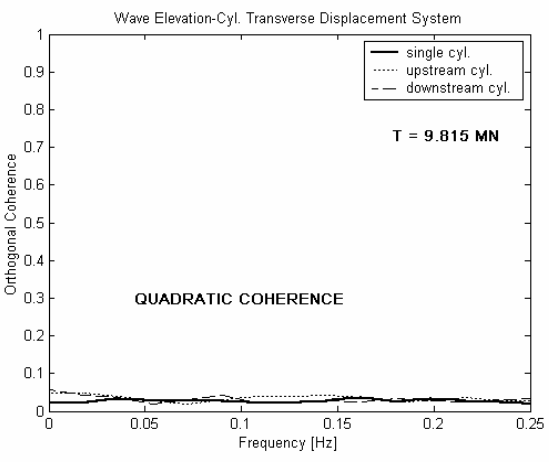

(e)

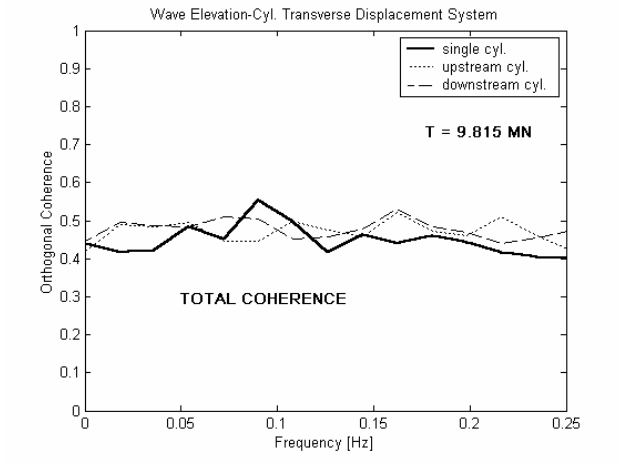

(c)

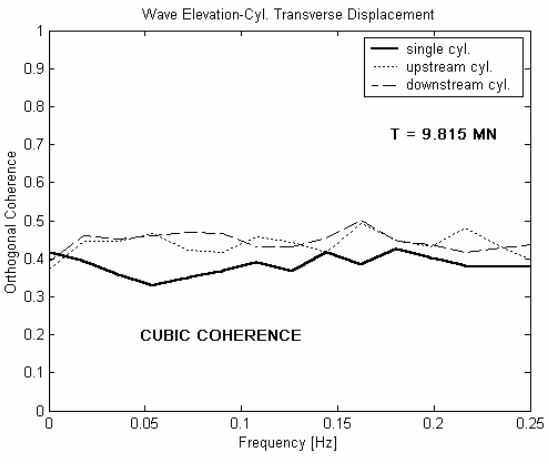

(f)

Figure 5. Volterra Modeling Results for Wave Elevation-Transverse Cyl. Displacement Systems; T=9.815 MN.

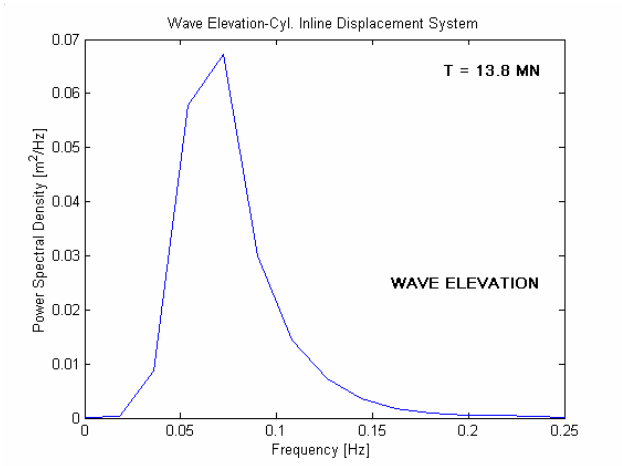

(a)

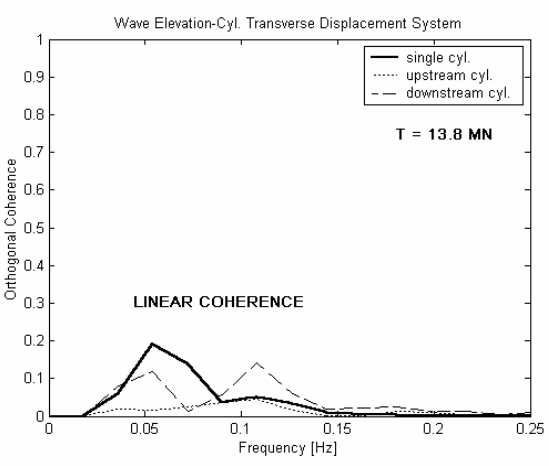

(d)

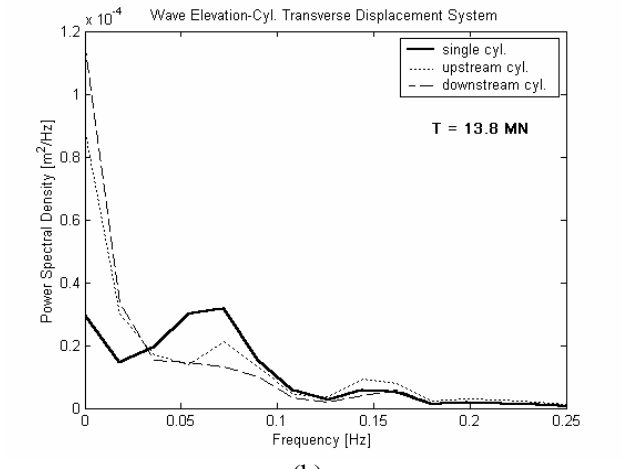

(b)

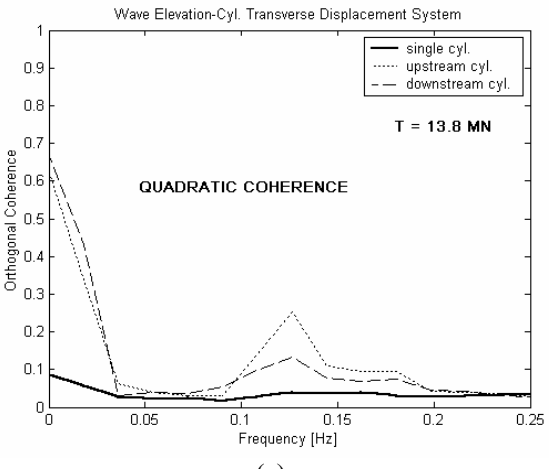

(e)

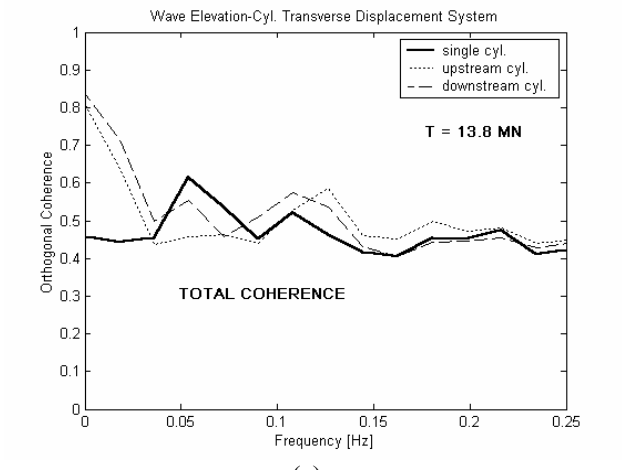

(c)

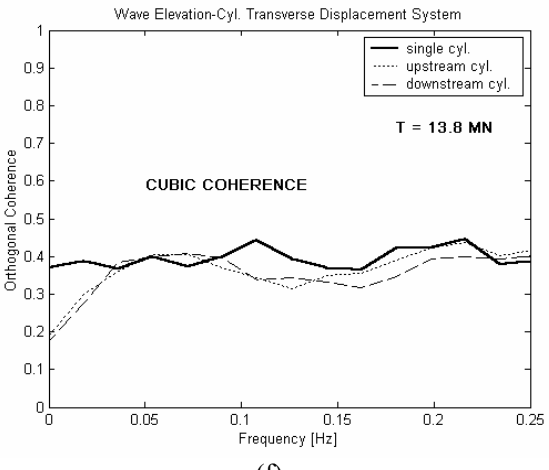

(f)

Figure 6. Volterra Modeling Results for Wave Elevation-Transverse Cyl. Displacement Systems; T=13.8 MN.

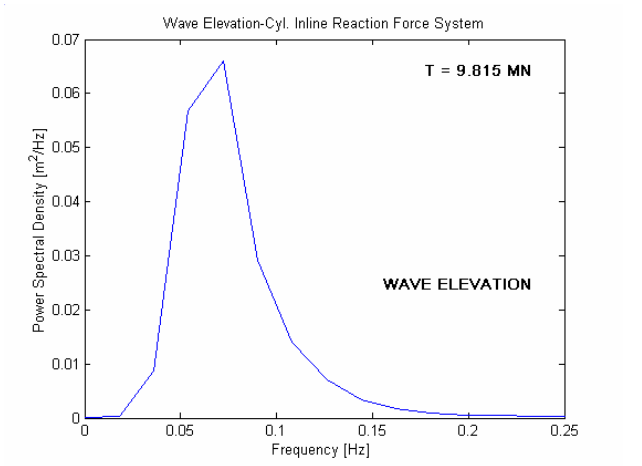

(a)

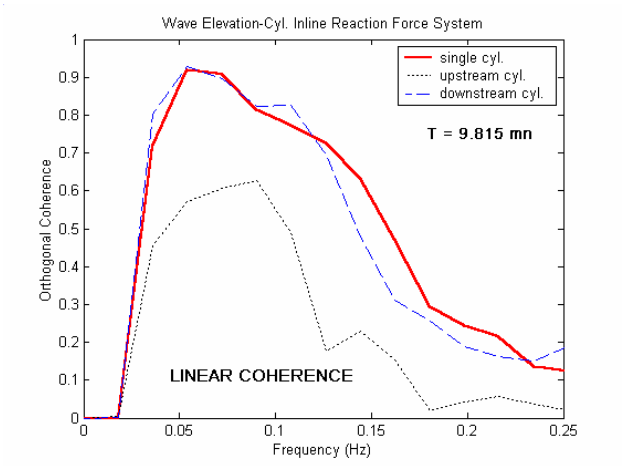

(d)

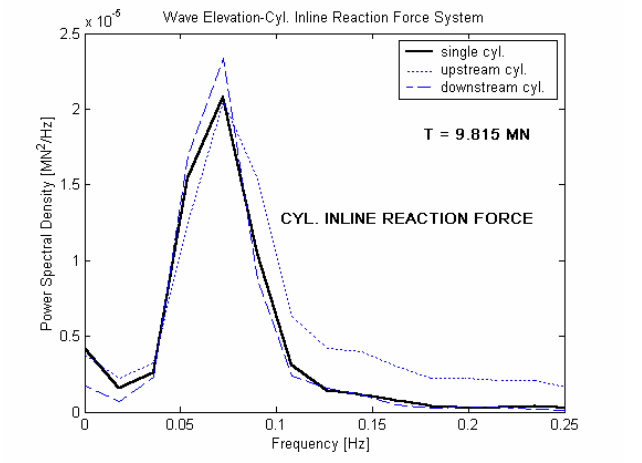

(b)

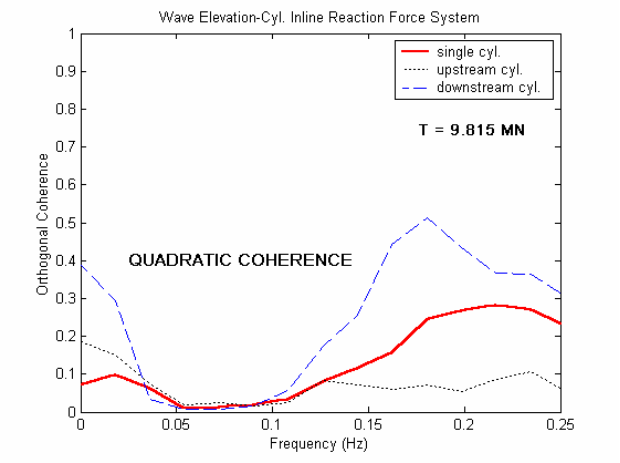

(e)

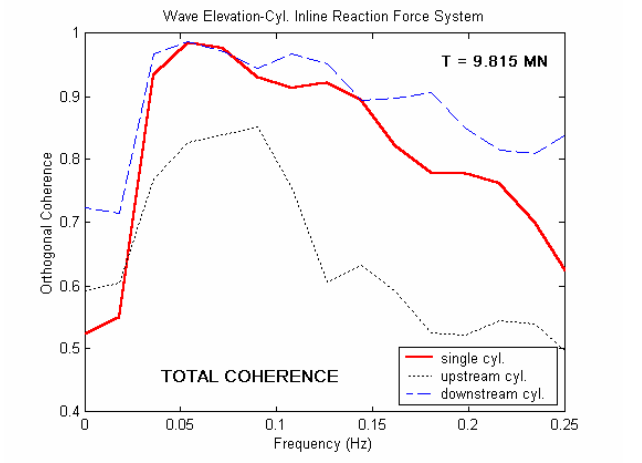

(c)

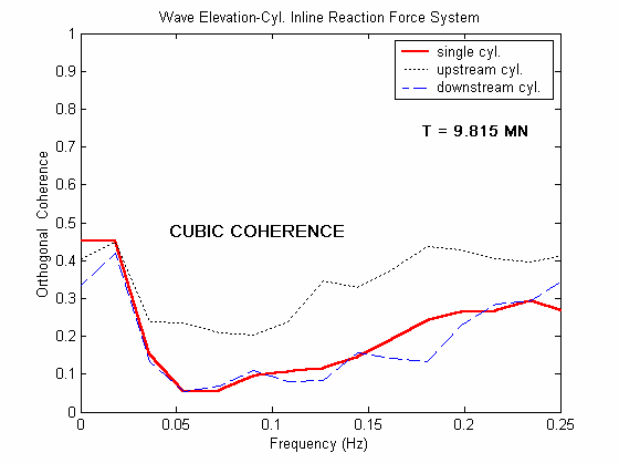

(f)

Figure 7. Volterra Modeling Results for Wave Elevation-Cyl. Inline Reaction Force Systems; T=9.815 MN.

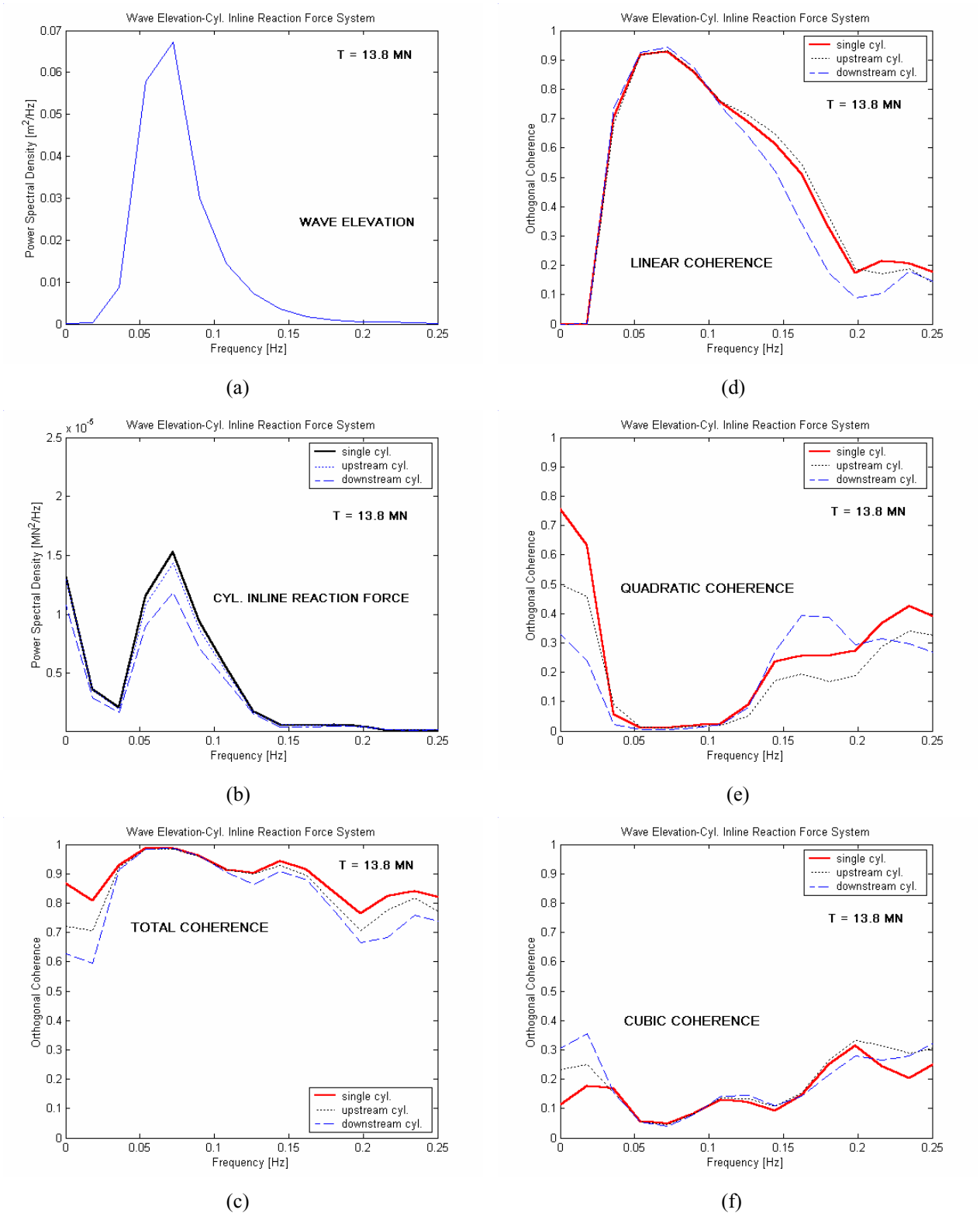

Figure 8. Volterra Modeling Results for Wave Elevation-Cyl. Inline Reaction Force Systems; T=13.8 MN.

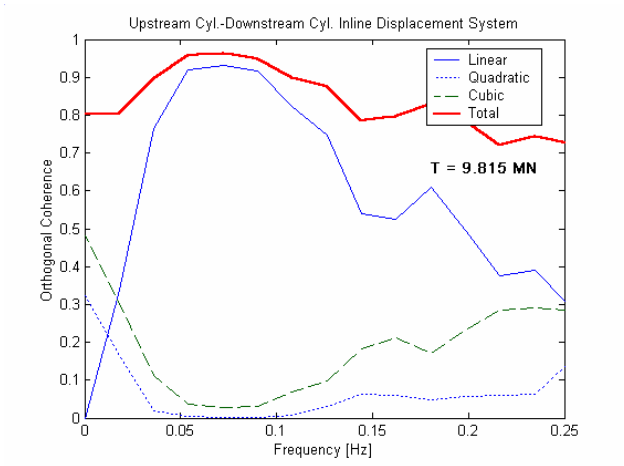

(a)

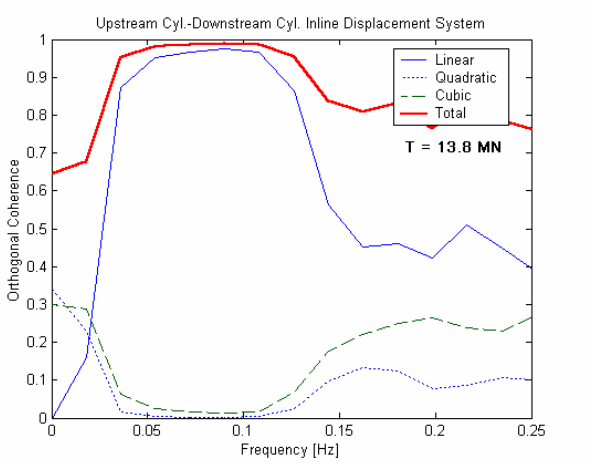

(d)

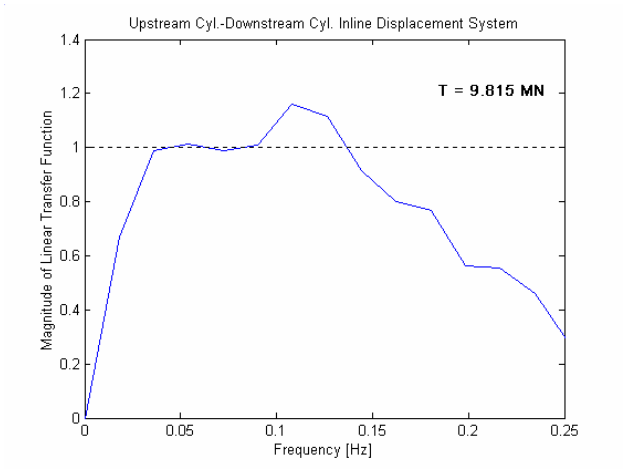

(b)

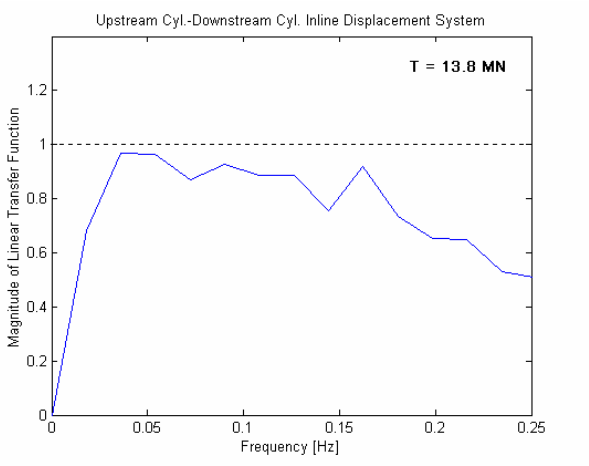

(e)

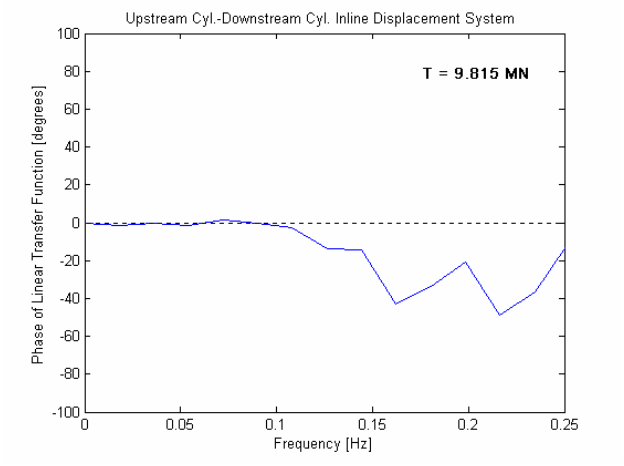

(c)

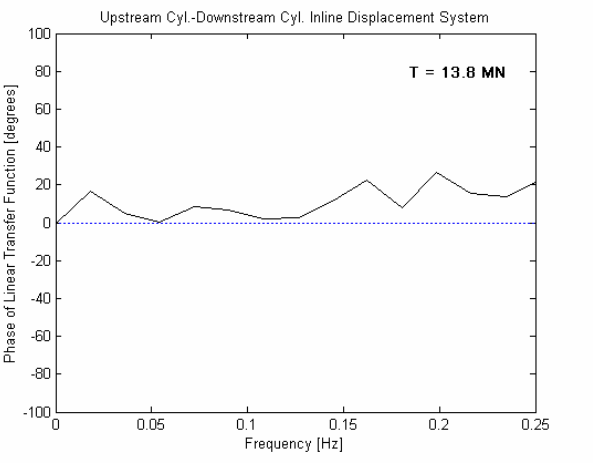

(f)

Figure 9. Volterra Modeling Results for Upstream Cyl.- Downstream Cyl. Inline Displacement System.

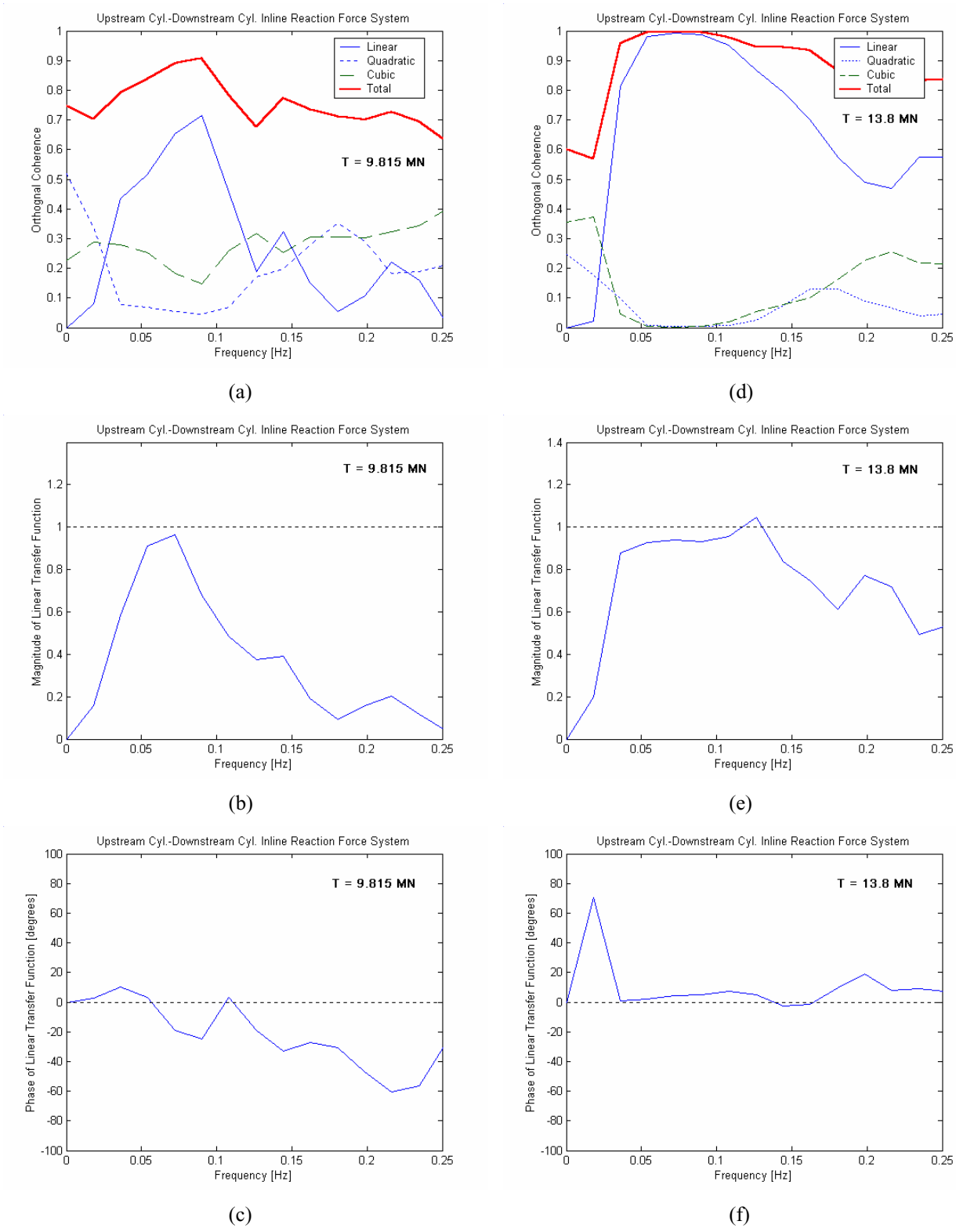

Figure 10. Volterra Modeling Results for Upstream Cyl.- Downstream Cyl. Inline Reaction Force System.